Environmental Science & Technology

Article

pubs.acs.org/est

Predictive Modeling of Subsurface Shoreline Oil Encounter Probability from the Exxon Valdez Oil Spill in Prince William Sound, Alaska

Zachary Nixon* and Jacqueline Michel

Research Planning, Inc. 1121 Park Street, Columbia, South Carolina 29201, United States

Supporting Information

ABSTRACT: To better understand the distribution of remaining lingering subsurface oil residues from the *Exxon Valdez* oil spill (EVOS) along the shorelines of Prince William Sound (PWS), AK, we revised previous modeling efforts to allow spatially explicit predictions of the distribution of subsurface oil. We used a set of pooled field data and predictor variables stored as Geographic Information Systems (GIS) data to generate calibrated boosted tree models predicting the encounter probability of different categories of subsurface oil. The models demonstrated excellent predictive performance as evaluated by cross-validated performance statistics. While the average encounter probabilities at most shoreline locations are low across western PWS, clusters of shoreline locations with elevated encounter probabilities remain in the northern parts of the PWS, as well as more isolated locations. These results can be applied to estimate the location and amount of remaining oil, evaluate potential ongoing impacts, and guide remediation. This is the first application of quantitative machine-learning based modeling techniques in estimating the likelihood of ongoing, long-term shoreline oil persistence after a major oil spill.

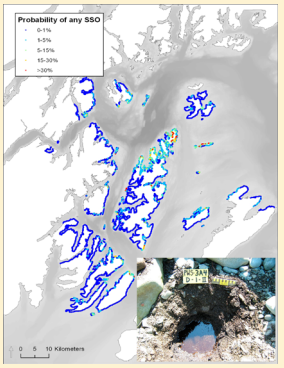

INTRODUCTION

Oil from the 1989 *Exxon Valdez* oil spill (EVOS) of 10.8 million gallons of Alaska North Slope crude oil still persists as surface and subsurface oil residues along the shorelines of Prince William Sound (PWS), Alaska, more than two decades after the spill. There is some evidence that this oil has potentially contributed to the long-term impact of the spill on certain species, including sea otters and harlequin ducks.[1] Short et al.[2] estimated that, in 2001, 7.8 ha (range of 4.06−12.7 ha) of subsurface oil remained in PWS, but did not specify where this oil might occur.

All previous quantitative investigations of subsurface oil (SSO) presence after the mid-1990s have relied upon conclusions drawn from site specific investigations. More explicit synoptic spatial predictions of the distribution of oil in the spill impact areas are required to determine the potential need for active restoration of sediments and associated resources and to evaluate the potential links between persistent oiling and recovery rates of injured resources. Because subsurface oil is difficult to detect, and because the shoreline landscapes affected by the EVOS are complex and extensive, an effective way of predicting the presence of subsurface oil is required to evaluate potential for ongoing impacts. Michel et al.[3,4] developed a set of predictive models for use in classifying shorelines as likely or unlikely to harbor subsurface oil, but the models were designed to predict locations with remaining subsurface oil by calculating a class-membership score for all shoreline locations. Detailed assessments of the potential for ongoing impact require actual subsurface oil encounter probabilities.

This work furthers the work of Michel et al.[3,4] and presents a suite of calibrated boosted tree models developed to make spatially explicit predictions about the probability of encountering different categories of subsurface oil sequestered in the intertidal subsurface in excavated pits based upon field data and synoptic predictor variables. This is, to our knowledge, the first application of quantitative models in general, and machine-learning based modeling techniques, in estimating the likelihood of shoreline oil persistence after a major oil spill.

MATERIALS AND METHODS

Many studies have identified factors that affect the behavior and persistence of oil on the shorelines of PWS and the Gulf of Alaska in the more than 20 years since the spill.[2−12] As part of these studies, the presence of both surface and subsurface oiling and the presence of geomorphic factors that led to oil persistence have been documented at discrete locations; however, these studies are largely descriptive, and limited quantitative extrapolation was possible. We used survey data describing the presence of subsurface oil in excavated pits together with synoptic predictor variables to derive a series of models for use in generating calibrated probabilities of encountering subsurface oil of various types at all locations.

Physical Setting. PWS is a semienclosed sound in south-central Alaska with a convoluted and fjorded coastline. Surficial

Received: November 13, 2014
Revised: February 18, 2015
Accepted: February 26, 2015
Published: February 26, 2015

DOI: 10.1021/es502579u
Environ. Sci. Technol. 2015, 49, 4354−4361

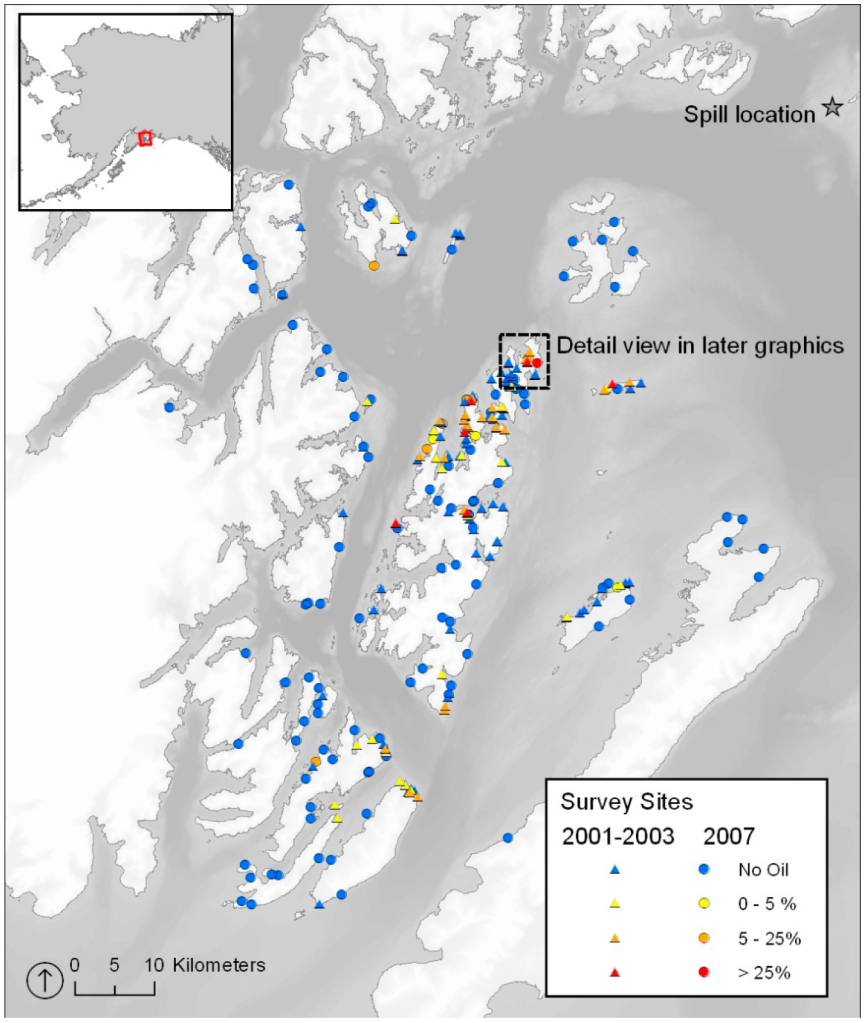

Figure 1. Location map of Prince William Sound, AK with survey sites investigated for the presence of subsurface oiling in 2007[3] and 2001−2003[2,19] symbolized by the percentage of excavated pits with SSO detected. Box in dotted line depicts extent of later detailed graphics in Supporting Information.

geology is complex and includes intermixed sedimentary, metasedimentary, volcanic, and granitic rocks.[3,13] Winds in the PWS region are also complex, with a wide range of prevailing wind directions and strongly influenced by local topography.[14] Storm winds are generally from the southeast−east-northeast.[15] Average open-water significant wave heights in mid-PWS are 0.7 m with a maximum significant wave height of 4.5 m over the period between 1995 and 2001[15] though many inlet and fjord interiors are sheltered from significant wave exposure. Tides are semidiurnal with a range of 5.5 m. Average annual sea surface temperature (°C) ranges from 0° to 20.4° with an average of 8.8°.[15] Open water surface currents velocities can be as high as 150 to 200 cm/s and large tidal ranges generate surface currents of similar magnitude at local scales in straights and entrances.[16−18]

Field Data. We used the pooled data set of excavated pit survey described in Michel et al.[3] composed of fieldwork by those authors in 2007 as well as field data described in Short et al.[2,19] from 2001 and 2003 (Figure 1). All field data were collected using the methods described in Short et al.[2] Shoreline segments were examined for surface and subsurface oil using a stratified-random method. Briefly, shoreline segments at sampling locations were partitioned into areal units based on along-shore lengths and tidal elevation and randomly located 0.25 m^2 pits within those units were excavated to a depth of 0.5 m and examined for the presence of subsurface oil. All observed oil was categorized and described using standardized descriptors compatible with those used previously in PWS and described by Gibeaut and Piper[20] including oil Film (OF), Light Oil Residue (LOR), Medium Oil Residue (MOR), and Heavy Oil Residue (HOR). We used this compiled database of field data containing data describing 13,743 subsurface pits excavated across the beaches of PWS between 2001 and 2007. Of these, 507 pits (3.7%) had subsurface oil present.

Predictor Variables. Review of previous investigations[2−12] indicated that the primary drivers of control of long-term oil persistence after oil has been stranded are initial oil loading, shoreline geometry and geomorphology, and wind wave exposure. Based on this review, we derived a series of raster layers describing oiling and physical variables thought to influence and control the presence and persistence of subsurface oil in PWS. In contrast to recent investigations of behavior of recently stranded oil on shorelines in other settings[21,22] climactic and oceanographic variables describing more homogeneous or less energetic physical processes including surface currents, seawater characteristics, and surface currents are not thought to play a significant role in oil

DOI: 10.1021/es502579u
Environ. Sci. Technol. 2015, 49, 4354−4361

persistence in PWS many decades after oil stranding, and were not included in modeling efforts.

We first calculated a series of estimates of shoreline surface oil loading per unit shoreline length from historical shoreline oiling survey data[23,24] collected by Shoreline Cleanup and Assessment Technique (SCAT) teams. These data consist of categorical oiling descriptors of heavy, medium, and light that describe surface oiling conditions along shoreline line segments. Historical SCAT oiling was available for fieldwork conducted during the fall of 1989, spring of 1990, and spring of 1991. The categorical descriptors used in these data were derived from the application of a heuristic matrix to multiple, more quantitative field measurements, such as estimated width of oil band and percent cover. We converted these categorical descriptors to numeric values by taking the midpoint of the range of reported values for across-shore oiled bandwidth multiplied by the midpoint of the range of reported values of percent cover for that band. This yielded numerical estimates in units of m^2/m ranging from 0 for no oil observed to 5.63 m^2/m for heavy oiling in 1990 and 1991. An index of oiling was created by averaging estimated shoreline surface oil loads within a circular moving window with a 50 m radius. These averaged values accounted for both the spatial inaccuracies inherent in the original data, and those introduced by the need to reference all data together.

Shoreline geomorphology is known to have a strong relationship with deposition and persistence of stranded oil both in PWS[6] and in the Gulf of Alaska.[9,10] We included a suite of variables representing shoreline morphology based upon shoreline geometry, near-shore topography, and shoreline geomorphic classification data. Shoreline geometry is known to influence the wave and current energy incident upon a shoreline and, thus, may affect the deposition and persistence of stranded oil. We incorporated shoreline geometry using a continuous index of concavity/convexity calculated for each 10 m cell representing the shoreline. We calculated this index, for each cell, as the mean of all cells within a given radius in a land/water raster grid wherein cells were coded as zero for water and one for land. This yielded a unit-less index ranging from near zero (extremely convex) to near one (extremely concave). This index was calculated using multiple radii (50, 100, and 500 m) representing convexity/concavity at three different spatial scales.

We derived surface slope and rugosity predictor variables from a topographic/bathymetric digital elevation model (DEM). We obtained topographic DEM data from NOAA[25] and supplemented with additional bathymetric data from NOAA.[26] All DEM rasters were converted to points, converted to a mean sea level (MSL) vertical datum and an integrated bathymetric/topographic surface was created using the TOPOGRID procedure forcing the resulting surface through the shoreline in ArcGIS.[27] Slope in degrees was calculated for each cell representing land using an eight-direction, 3 × 3 cell moving-window method. We calculated a measure of topographic complexity similar to rugosity or surface roughness using a method modified from Hobson.[28] This index was calculated as the diversity of topographic aspect within a circular moving window with a 50 m radius applied to the integrated bathymetric/topographic DEM.

We obtained NOAA Environmental Sensitivity Index (ESI) data[29,30] describing shoreline morphology in the region. These data classify the shoreline into consistent morphological units and assigns ranks based on relative sensitivity to oil. Previous investigation[3] indicated that shoreline morphological class alone was a poor predictor of oil presence because there are many examples of both oiled and unoiled locations within any given class. Interfaces between permeable and impermeable portions of the shoreline often were associated with aggregations of subsurface oil.[3,4] As such, a measure of morphologic complexity was calculated as the distance in meters to an interface between a permeable and impermeable unit derived from NOAA ESI data. Additionally, an impermeability index was derived using values from actual field data wherein permeability was defined as the percentage of pits at all locations with a given single ESI class where any permeable substrate was successfully excavated using hand tools (see Table T1, Supporting Information). For locations with multiple cross-shore ESI classes, permeability was defined as the average of the constituent single-class permeability values in that multiple-value class.

Exposure to wave energy is an important factor controlling the persistence of oil on many types of shorelines. We evaluated shoreline exposure to wave and current energy using measures of average fetch in kilometers, as well as a unitless exposure index. We used climatological summary data from 1995 to 2001 from NOAA data buoy 46060[30] as the best representative data set for evaluating winds in the area of interest. This data buoy is located in open water in the center of PWS, closest to the area of interest, but not affected by local topographic effects. These effects can be large in PWS, but no other long-term data sets exist.

We calculated fetch as a raster operation in ArcGIS according to the USACE[31] modified effective fetch calculation methodology. This method calculates fetch in a given direction as the arithmetic mean of the overwater length of nine radials around that direction at 3-degree increments. Inputs to the operation consisted of a land-water grid with a 100 m cell size, wherein fetch length is calculated for each open water grid cell. All cells were assigned a maximum fetch of 100 km in any given direction. This method of calculating fetch utilized methods and code for ArcGIS made available by Rohweder et al.[32] A cell size of 50 m was used for fetch and related operations. We created an exposure index using the fetch grids using methods modified from Hayes.[14] We generated wind statistics (see Figure S1 in Supporting Information) of cumulative frequency of wind speed in knots by direction in two classes: 10−20 knots and greater than 20 knots. In PWS, the majority of winds greater than 10 knots in velocity blow from between 90 and 120 degrees. An exposure index was then calculated for all open water and alongshore locations as

$$\mathrm{EI} = \sum_{i=1}^{12} \left(F_i \times [P_i \times 10]\right) + \left(F_i^{*}[\mathrm{Ps}_i \times 10]^2\right)$$

where EI is a unitless index of wave exposure, i is the wind direction, F_i is modified effective fetch as calculated in direction i in kilometers, P_i is the cumulative percentage of time the wind blows between 10 and 20 knots from direction i, and Ps_i is the cumulative percentage of time the wind blows at greater 20 knots from direction i.

Overwater distance to stream mouths was also included as a predictor variable. The presence of stream or river mouths has been noted by some authors as a potential reservoir for spilled oil along the shoreline.[21,22] Other authors[3,12] have noted that the high flow and steep gradient of most streams in PWS generate alluvial fan deposits in the intertidal where high

DOI: 10.1021/es502579u
Environ. Sci. Technol. 2015, 49, 4354−4361

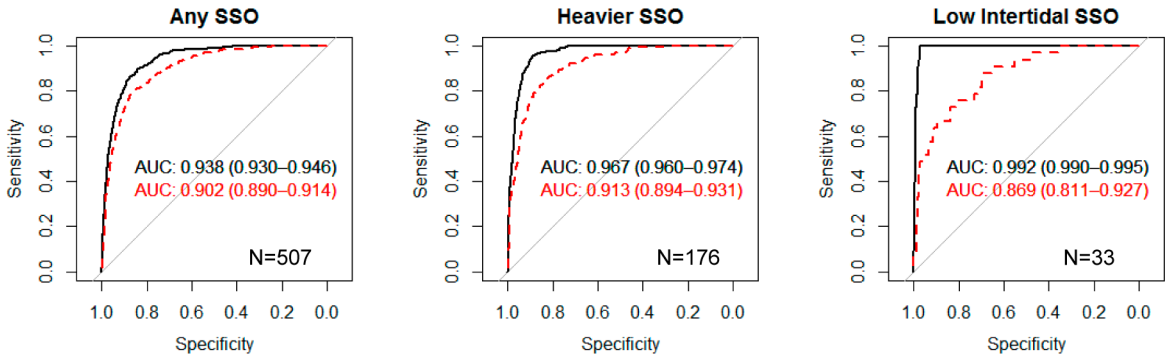

Figure 2. Receiver operator characteristic (ROC) curves and area under the curve (AUC) and 95% confidence intervals derived from training data (black) and 10-fold cross-validation (red) for predictive BRT models of pit-wise oiling presence for three different subsurface oiling types. Count of pits with observed oiling types indicated.

porosity and groundwater flow lead to removal of most subsurface oil. Distance was calculated as Euclidean overwater distance to vector stream mouths derived from Chugach National Forest data.[33]

Two additional proxy variables that are thought to be related to oiling history were included. These were the overwater distance to the spill site and a measure of oil approach angle. Overwater distance to the spill site was calculated as Euclidean least accumulative overwater distance to the spill origin. Also, an index related to the angle of overwater−oil approach relative to the shoreline orientation was created. This index was thought to be important in that locations where the shoreline was oriented normal to the angle of oil approach were thought to be more likely to accumulate and retain subsurface oil. This index was created by calculating both the shore-normal angle for every location along the shoreline, and the estimated angle of oil approach as the aspect of the least accumulative overwater distance grid as described above. The index (I) was calculated for each cell as

$$I = \frac{\cos(O - A) + 1}{2}$$

where O is the angle of oil approach and A is the angle normal to the shoreline.

All predictor variables were generated for cells in a 10 m by 10 m raster grid representing a linear shoreline for all locations with at least one SCAT survey (see Figure S2 in Supporting Information).

Model Development. We assigned all pits the values of the oiling history and physical predictor variables at their respective shoreline locations. We then used these data to generate three different predictive models estimating:

1. The pit-wise encounter probability for any subsurface oil at a given alongshore location ("Any SSO")
2. The pit-wise encounter probability for subsurface oil categorized as MOR or HOR at a given alongshore location ("Heavier SSO")
3. The pit-wise encounter probability for any subsurface oil at a given alongshore location at a tidal elevation lower than 1.5 m above MLLW ("Low intertidal SSO")

Tree-based models recursively partition the predictor variable space into regions using fixed rules to best assign each region to a class or value, and can simply include nonlinearities and interactions among multiple predictors. Boosted regression trees (BRTs) generate an ensemble of tree-based models rather than a single model.[34] Boosting is similar to model averaging, but operates in an iterative sequential manner.[35,36] Tree-based models are fitted iteratively to gradually increase emphasis on observations poorly modeled by previous trees. Elith et al.[37] provide a review of steps involved in application of BRTs to real-world prediction problems. We used the *step.gbm* functions of Elith et al.[37] which in turn makes used of the gbm package[38] all as implemented in the dismo package.[39] We used a bag fraction of 0.8, a learning rate of 0.01, and a maximum tree complexity of 3. These parameters were determined via trial and error to produce the best trade-off between model performance and computational efficiency. All other parameters were set to default software settings. We included all evaluated predictor variables as inputs to the BRT models because of the ability of this method to more rigorously select from competing predictors, and remove unimportant ones. The relative importance of each variable in the shoreline oil presence models was evaluated by computing the reduction in deviance attributable to each variable in predicting the gradient of the following iteration, and presented as the relative influence of each variable in reducing the loss function.[34] The marginal effect of each variable was then plotted, depicting the effect of that variable with other variables integrated out to evaluate the effects of individual variables.

We evaluated the performance of these models by computing the area under the curve (AUC) of the receiver operator characteristic (ROC) curve plots[40,41] both for all the data used to train the model, and for a 10-fold cross validation, wherein the data are divided into 10 parts, stratified by prevalence, and a separate model is trained on 90% and tested on the remaining 10%. ROC curves and AUC statistics were computed using the *pROC* package.[42] BRT models generally perform much better than many other methods as a binary classifier, but often not as well as an estimator of the true class probability.[43,44] As such, we calibrated the BRT model output to yield true encounter probabilities based on the scaling method of Platt[45,46] using the out-of-sample cross-validation folds from the *gbm.step* procedure.

After model calibration, we generated calibrated pit-wise shoreline subsurface oil encounter probabilities for each cell in a 10 m by 10 m raster grid representing all shoreline locations potentially exposed to oil. Any shoreline location surveyed by the SCAT program in any year was considered to have been potentially exposed to oil. Each 10 × 10 m raster cell is equivalent to a length of 7.3 m, derived from the total number of shoreline raster cells in the data set and the total length of the NOAA ESI vector shoreline in the data set.[29] A total of

DOI: 10.1021/es502579u
Environ. Sci. Technol. 2015, 49, 4354−4361

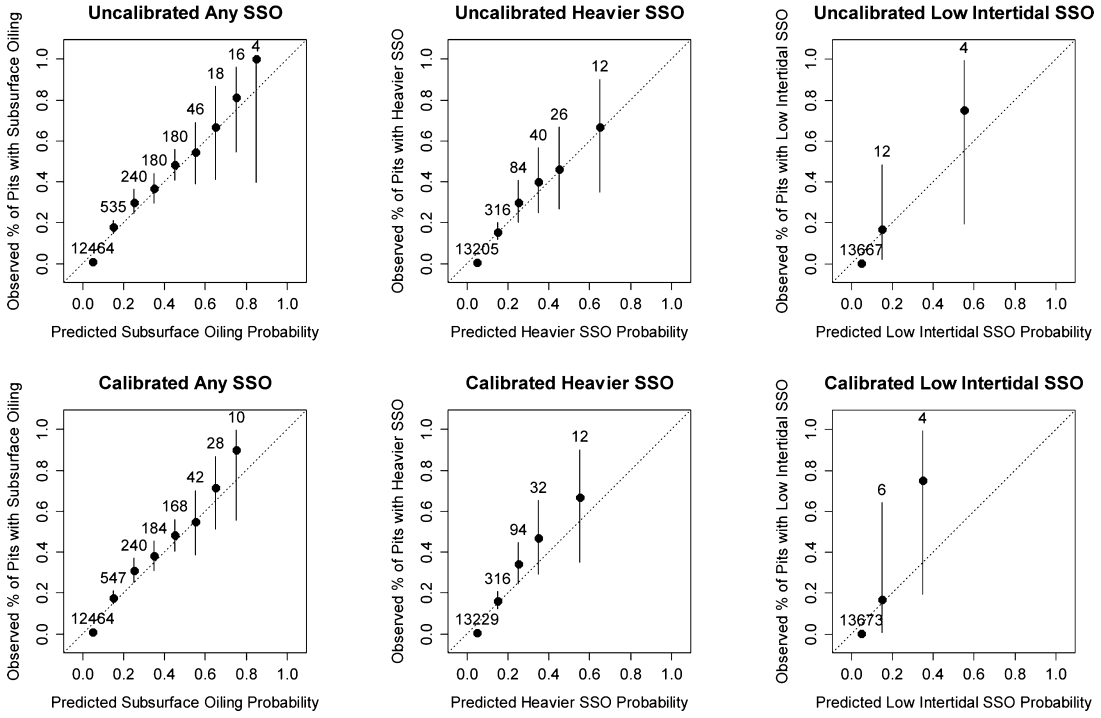

Figure 3. Calibration plots of observed versus predicted values for boosted classification tree models of pit-wise oiling presence for three different subsurface oiling types before and after calibration via Platt scaling. Each plot displays average observed prevalence (dot) and confidence intervals (bars) within bins defined by predicted probabilities. Number of observations in each bin is noted.

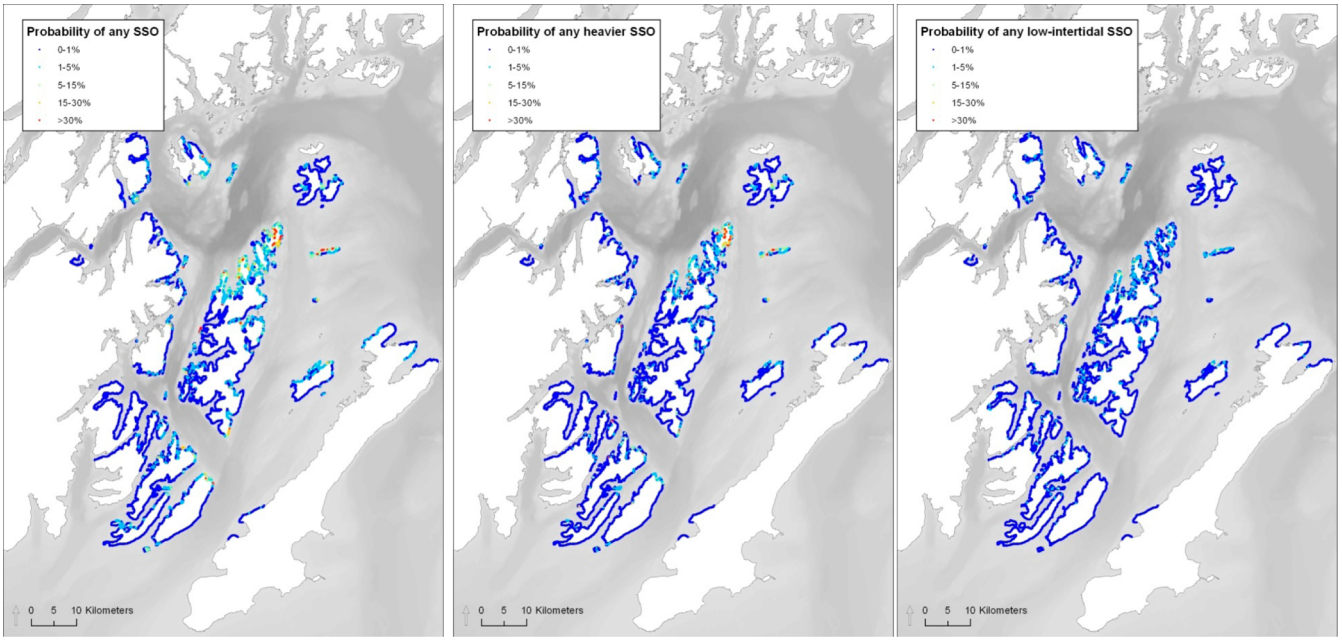

Figure 4. Model estimated pit-wise shoreline subsurface oil (SSO) encounter probabilities for any type of SSO (left), heavier SSO (middle), and SSO in the lower intertidal (<1.5 m above MLLW, right) for locations spaced along the shoreline every 10 m.

171 872 shoreline cells were included for analysis, depicting approximately 1255 km of shoreline.

RESULTS

The BRT models of the presence of shoreline oiling of different classes yielded cross-validated AUC values of AUC curves (Figure 2) near or above 0.9 for each model implying very good performance.[40]

Calibration success appears mixed in the calibration plots (Figure 3) before and after Platt scaling, particularly for pits with higher predicted probabilities of SSO presence overall. However, because the prevalence, or number of observed pits in the data set with the subsurface oiling of the specified type is so small relative to the overall number of pits, small improvements in estimated probabilities for pits with overall low probabilities will yield dramatically better calibration overall, even if probabilities for pits with higher probabilities

DOI: 10.1021/es502579u
Environ. Sci. Technol. 2015, 49, 4354−4361

are unchanged or worsened.[47] For this application, however, we are seeking the best calibrated estimates across all locations, and the large majority of locations had very low probabilities of encountering SSO of any kind so this is of lesser concern.

Marginal response curves and relative importance values for each predictor variable (see Figure S3 in Supporting Information) were inspected for all three models to evaluate the contributions of individual predictors. For both the all SSO and heavier SSO models, relative variable importance and marginal response are similar. Generally, distance to spill and surface oil loading in 1991 are the two single most important predictors, with those two variables contributing over 40% of the explanatory power in the model. The precise ordering of the remaining predictors in importance differs somewhat between the two models, but they are fairly similar and the shape of the marginal response curves is also similar. The lower intertidal SSO model, by contrast, displays both substantive differences in variable importance from the first two models, but also some notable differences in marginal responses as well. The distribution of lower intertidal SSO is less related to oil loading observed in 1991, with that variable contributing less than 5% toward the explanatory power of the model and with predicted lower encounter probabilities for this type of SSO with higher observed surface oil loading in 1991.

Mapped model results for all shorelines (Figure 4) reveal distinct patterns to the predicted distribution of SSO encounter probabilities. Average predicted calibrated pit-wise shoreline subsurface oil encounter probabilities over all shoreline locations were low: 0.007, 0.003, and 0.002 for the any SSO, heavier SSO, and low-intertidal SSO model variants, respectively. Significant hotspots exist in the output, however, where maximum predicted encounter probabilities were 0.76, 0.87, and 0.36 for any SSO, heavier SSO, and low-intertidal SSO model variants, respectively. Shoreline locations with elevated encounter probabilities were located on northern Knight Island, Disk Island, Eleanor Island, and Smith Island, as well as more isolated sets of locations in Green Island, southern Knight Island, and other locations on the southern portion of the study area. Total estimated shoreline lengths by model variant SSO encounter probability also range widely (Table 1) with 177.4 km estimated to have an encounter probability of any SSO of greater than 1%, but only 100 m of shoreline estimated to have an encounter probability of greater than 25% for oil in the low intertidal.

Table 1. Estimated Lengths of Shorelines in Western PWS with Model Estimated Pit-Wise Shoreline Subsurface Oil (SSO) Encounter Probabilities above Three Cutoff Levels for Any Type of SSO, Heavier SSO, and SSO in the Lower Intertidal (<1.5 m Above MLLW)

model	>1%	>5%	>25%
any subsurface oil	177.4 km	26.0 km	2.0 km
heavier subsurface oil	60.2 km	9.0 km	0.8 km
subsurface oil in lower intertidal (<1.5 m above MLLW)	29.2 km	3.1 km	0.1 km

DISCUSSION

The machine learning algorithms used to generate the models presented here appear to provide improvements in performance over traditional modeling methods, similar to those observed in other modeling settings. Specifically, we find that these models were able to generate accurate and well-calibrated estimates of the pit-wise encounter probability of different types of subsurface oiling across PWS. In all cases the AUC values as derived from cross-validation are lower that the training data, as expected. The AUC value as derived from cross-validation for the low intertidal SSO model demonstrates the largest decrease from the training data derived value, implying potential overfitting. Given the very small number of pits in the low intertidal with SSO we would expect any model using a subset of positive training samples would have both a reduced AUC and greater variability in AUC results when compared to a model parametrized using the entire data set.

The model predictor relative importance and marginal effect curves (Figure S3 in Supporting Information) also have implications more generally for understanding controls on long-term oil persistence for this and, potentially, other spills. For the SSO and heavier SSO model variants, model predictor importance was very similar. Distance to spill and oil loading in 1991 were the strongest predictors of present day oil persistence indicating that near-term persistence of heavier surface oil is a good indicator of long-term persistence of subsurface oil. By contrast, wind wave exposure and fetch are relatively weak predictors of the probability of presence of these two types of subsurface oil. While initially surprising when compared with Hayes et al.,[14] or Adler and Inbar[21] this reinforces the conclusions of previous investigations[12] which argue for the existence of a more complex relationship between wave exposure and geomorphology, particularly for long-term subsurface oil persistence. Other authors[11] have described locations that harbor heavier persistent subsurface oil as typically being located in areas with heavy initial oil loading, and generally located in areas of localized sheltering within the beach face and associated with finer grained sediments, and these model results generally reflect these observations.

Of note is that the shoreline convexity at the 50 m scale was a relatively important predictor for all SSO models—with more concave locations more likely to harbor lingering subsurface oil regardless of SSO type or wave exposure. To our knowledge, the use of shoreline geometry to predict oil persistence along shorelines has not been previously attempted. Similarly, topographic slope as evaluated with the DEM used here appeared to have been a moderately powerful predictor of subsurface oil presence with increased probability of SSO presence at locations with slopes of 25° and 35° for any SSO and heavier SSO, and above 25° for SSO in the lower intertidal. Nixon et al.[12] previously found that the presence of persistent subsurface oil is related to lower intertidal angle only at more exposed locations. At more sheltered locations, higher angle shorelines can harbor lingering subsurface oil. While methods used to measure slope differ, these results imply similar processes.

The apparent differences in predictors of lower intertidal SSO as compared with other the other two models were significant. The most important predictors for this type of subsurface oil were slope and distance to spill, with historical shoreline surface oil loading not included in the top two predictor variables. Subsurface oil in the lower intertidal was generally encountered in sheltered locations, sequestered in fine-grained sand and gravel at the toe of relatively steep, concave pocket beaches with no surface armoring. In these locations, it is likely that surface oil and subsurface oil would have been removed from middle intertidal locations more rapidly due to increased wave exposure and lack of armoring.

DOI: 10.1021/es502579u
Environ. Sci. Technol. 2015, 49, 4354−4361

The permeability and geomorphic complexity variables derived from geomorphologic shoreline classifications in the NOAA ESI data[29] were relatively weak predictors of long-term subsurface oil persistence. We hypothesize that permeability, as defined here based upon a classified shoreline with a minimum mapping unit of significantly greater than 50 m, is simply not precise enough for evaluating the likelihood of the presence of an envelope of sediment suitable to harbor subsurface oil at the scale of a single 0.25 m^2 pit. Similar confounding scale issues are also likely affecting the utility of the geomorphic complexity index. We also note that the ESI ranking[30] is based primarily around behavior of stranded oil on shorelines on time scales of spill response (weeks and months) while the factors that control where oil that persists in PWS 25 years after the spill are much different. As such, these results have few implications for the utility of ESI data in general.

While the linkages between the data used and the physical phenomena that drive persistence are not always clearly understood, the performance of these models is remarkably good. The model results make explicit the distribution of the shoreline locations in western PWS that are likely to contain lingering subsurface oil. These locations are limited but significant in extent, and strongly clustered in certain locations. These results have direct application in evaluating the potential links between persistent oiling and recovery rates of injured resources, as well as evaluating the need for potential active restoration efforts. While it is important to note that these models are intended specifically for use in PWS, and may not generalize well to other spills or settings, the powerful predictive performance achieved suggests that these techniques deserve to be included in the toolbox of the applied coastal geomorphology and oil spill response communities.

■ ASSOCIATED CONTENT

Supporting Information

Supporting Information includes additional tables and graphics describing shoreline permeability estimates, wind climate statistics and buoy location map, example maps of all predictor variables, and plots of marginal effects and relative variable importance of included model variables. This material is available free of charge via the Internet at http://pubs.acs.org/.

■ AUTHOR INFORMATION

Corresponding Author

*Phone: 803-256-7322; fax: 803-254-6445; e-mail: znixon@researchplanning.com.

Notes

The authors declare no competing financial interest.

■ ACKNOWLEDGMENTS

The research described in this paper was supported by the Exxon Valdez Oil Spill Trustee Council. However, the findings and conclusions presented by the author(s) are their own and do not necessarily reflect the views or position of the Trustee Council. Peter Hagen served as the project coordinator. Mandy Lindeberg, Jeep Rice, and Mark Carls of the NOAA Auke Bay Laboratory (ABL) are acknowledged for their help in all phases of the work. Jeff Short and Jerry Pella are thanked for their invaluable assistance in study design.

■ REFERENCES

(1) Peterson, C. H.; Rice, S. D.; Short, J. W.; Esler, D.; Bodkin, J. L.; Ballachey, B. E.; Irons, D. B. Long-term ecosystem response to the *Exxon Valdez* oil spill. *Science* **2003**, *302*, 2082−2086.

(2) Short, J. W.; Lindeberg, M. R.; Harris, P. M.; Maselko, J. M.; Pella, J. J.; Rice, S. D. Estimate of oil persisting on the beaches of Prince William Sound 12 years after the *Exxon Valdez* oil spill. *Environ. Sci. Technol.* **2004**, *38* (1), 19−25.

(3) Michel, J.; Nixon, Z.; Hayes, M. O.; Short, J.; Irvine, G.; Betenbaugh, D.; Boring, C. *Modeling the Distribution of Lingering Subsurface Oil from the Exxon Valdez Oil Spill*, EVOS Restoration Project Final Report; 070801; Exxon Valdez Trustee Council: Anchorage, AK. 2009.

(4) Michel, J.; Nixon, Z.; Hayes, M. O.; Irvine, G.; Short, S. The Distribution of lingering subsurface oil from the Exxon Valdez Oil Spill. In *Proceedings of the 2011 International Oil Spill Conference*, Portland, OR, May 23−26, 2011; American Petroleum Institute: Washington, DC, 2011; pp 1−27.

(5) Jahns, H. O.; Bragg, J. R.; Dash, L. C.; Owens, E. H. Natural cleaning of shorelines following the Exxon Valdez spill. In *Proceedings of the 1991 International Oil Spill Conference*, San Diego, CA, March 4−7, 1991; American Petroleum Institute: Washington, DC, 1991. pp 167−176.

(6) Michel, J.; Hayes, M. O. *Geomorphological Controls on the Persistence of Shoreline Contamination from the Exxon Valdez Oil Spill*, NOAA Technical Report; HMRB 91-2; Hazardous Materials Response Branch: NOAA, Seattle, WA, 1991.

(7) Michel, J.; Hayes, M. O. Weathering patterns of oil residues eight years after the *Exxon Valdez* oil spill. *Mar. Pollut. Bull.* **1999**, *38*, 855−863.

(8) Owens, E. H. Shoreline conditions following the Exxon Valdez Spill as of fall. In *Proceedings of the Fourteenth Arctic and Marine Oil Spill Program Technical Seminar*, Vancouver, BC June 12−14, 1991; Environment Canada: Ottawa, ON, 1991. pp 579−606.

(9) Irvine, G. V.; Mann, D. H.; Short, J. W. Multi-year persistence of oil mousse on high-energy beaches distant from the *Exxon Valdez* spill origin. *Mar. Pollut. Bull.* **1999**, *38*, 572−584.

(10) Irvine, G. V.; Mann, D. H.; Short, J. W. Persistence of 10-year old *Exxon Valdez* oil on Gulf of Alaska beaches: The importance of boulder-armoring. *Mar. Pollut. Bull.* **2006**, *52*, 1011−1022.

(11) Taylor, E.; Reimer, D. Oil persistence on beaches in Prince William Sound—A review of SCAT surveys conducted from 1989 to 2002. *Mar. Pollut. Bull.* **2008**, *43*, 458−474.

(12) Nixon, Z.; Michel, J.; Hayes, M. O.; Irvine, G.; Short, J. Geomorphic factors controlling the persistence of subsurface oil from the *Exxon Valdez* Oil Spill. *J. Coastal Res., Spec. Issue.* **2013**, *69*, 115−127.

(13) Case, J. E., Barnes, D. F.; Plafker, G.; Robbins, S. L. *Gravity Survey and Regional Geology of the Prince William Sound Epicentral Region*, U.S. Geological Survey Professional Paper; 543-C; U.S. Geological Survey: Washington, DC, 1966.

(14) Hayes, M. O. An exposure index for oiled shorelines. *Mar. Pollut. Bull.* **1996**, *3* (3), 139−147.

(15) National Oceanic and Atmospheric Administration (NOAA) National Data Buoy Center (NDBC). Climatic Summary Tables [Online], 2007. http://www.ndbc.noaa.gov/ (accessed April 17, 2007).

(16) Wang, J. M.; Jin, E. V.; Patrick, J. R.; Allen, D. L.; Eslinger, C. N.; Mooers, K.; Cooney, R. T. Numerical simulations of the seasonal circulation patterns and thermohaline structures of Prince William Sound, Alaska. *Fish. Oceanogr.* **2001**, *10* (Suppl. 1), 132−148.

(17) Reed, R. K.; Schumaker, J. D. Physical oceanography. In *The Gulf of Alaska, Physical Environment and Biological Resources*; Hood, D. W., Zimmerman, S. T., Eds.; U.S. Government Printing Office: Washington, DC, 1986; pp 57−76.

(18) Royer, T. C.; Vermersch, J. A.; Weingartner, T. J.; Niebauer, H. J.; Muench, R. D. Ocean circulation influencing the *Exxon Valdez* oil spill. *Oceanography.* **1990**, *3*, 3−10.

DOI: 10.1021/es502579u
Environ. Sci. Technol. 2015, 49, 4354−4361

(19) Short, J. W.; Maselko, J. M.; Lindeberg, M. R.; Harris, P. M.; Rice, S. D. Vertical distribution and probability of encountering intertidal *Exxon Valdez* oil on shorelines of three embayments within Prince William Sound, Alaska. *Environ. Sci. Technol.* **2006**, *40*, 3723−3729.
(20) Gibeaut, J.; Piper, E. *1993 Shoreline Oiling Assessment of the Exxon Valdez Oil Spill*, EVOS Restoration Project Final Report; 93038; Exxon Valdez Trustee Council: Anchorage, AK, 1995.
(21) Adler, E.; Inbar, M. Shoreline sensitivity to oil spills, the Mediterranean coast of Israel: Assessment and analysis. *Ocean Coast. Manage.* **2007**, *50*, 24−34.
(22) Alves, T. M.; Kokinou, E.; Zodiatis, G. A three-step model to assess shoreline and offshore susceptibility to oil spills: The South Aegean (Crete) as an analogue for confined marine basins. *Mar. Pollut. Bull.* **2014**, *86*, 443−457.
(23) Teal, A. R. Shoreline cleanup—Reconnaissance, evaluation, and planning following the Valdez oil spill. In *Proceedings of the 1991 International Oil Spill Conference*, San Diego, CA, March 4−7, 1991; American Petroleum Institute: Washington, DC, 1991 pp 149−152.
(24) Neff, J. M.; Owens, E. H.; Stoker, S. W.; McCormick, D. M. Shoreline oiling conditions in Prince William Sound following the *Exxon Valdez* oil spill. In *Exxon Valdez Oil Spill: Fate and Effects in Alaskan Waters*; Wells, P. G., Butler, J. N., Hughes, J. S., Eds.; American Society for Testing and Materials: Philadelphia, PA, 1995; pp 312−346.
(25) Caldwell, R. J.; Eakins, B. W.; E. Lim, E. *Digital Elevation Models of Prince William Sound, Alaska: Procedures, Data Sources and Analysis*, NOAA Technical Memorandum; NESDIS NGDC-40; National Oceanic and Atmospheric Administration, Boulder, CO, 2011.
(26) National Oceanic and Atmospheric Administration (NOAA) National Geophysical Data Center (NGDC). National Ocean Service Hydrographic Data Base (NOSHDB). [Online], 2007, http://www.ngdc.noaa.gov/mgg/bathymetry/hydro.html (accessed on April 17, 2007).
(27) ESRI. *ArcGIS* v10.2. [Online], 2013, http://www.esri.com (accessed on August 20, 2013).
(28) Hobson, R. D. Surface roughness in topography: Quantitative approach. In *Spatial Analysis in Geomorphology*, Chorley, R. J., Ed.; Taylor & Francis: Methuen, London, 1972; pp 225−245.
(29) National Oceanic and Atmospheric Administration (NOAA) Office of Response and Restoration (ORR). Environmental Sensitivity Index for Prince William Sound, Alaska. [Online], 2000, http://response.restoration.noaa.gov/maps-and-spatial-data/download-esi-maps-and-gis-data.html (accessed on Aprile 17, 2007).
(30) National Oceanic and Atmospheric Administration (NOAA) Office of Response and Restoration. *Environmental Sensitivity Index Guidelines, version 3.0*, NOAA Technical Memorandum; NOS OR&R 11; National Oceanic and Atmospheric Administration: Seattle, WA, 2002.
(31) U.S. Army Corps of Engineers (USACE). *Coastal Engineering Manual*, Engineer Manual:; 1110-2-110; U.S. Army Corps of Engineers: Washington, D.C., 2002.
(32) Rohweder, J.; Rogala, J.; Johnson, B.; Anderson, D.; Clark, S.; Chamberlin, F.; Runyon, K. *Application of Wind Fetch and Wave Models for Habitat Rehabilitation and Enhancement Projects*, U.S. Geological Survey Open-File Report; 2008−1200; U.S. Geological Survey: Washington, DC, 2008.
(33) U.S. Department of Agriculture (USDA) Forest Service. Chugach National Forest freshwater streams. [Online], 2002, http://agdc.usgs.gov/ (accessed on April 13, 2006).
(34) Friedman, J. H.; Hastie, T.; Tibshirani, R. Additive logistic regression: A statistical view of boosting. *Ann. Math. Stat.* **2002**, *28* (2), 337−374.
(35) Friedman, J. H. Greedy function approximation: A gradient boosting machine. *Ann. Math. Stat.* **2001**, *29* (5), 1189−1232.
(36) Friedman, J. H. Stochastic gradient boosting. *Comp. Stat. Data Anal.* **2002**, *38*, 367−378.
(37) Elith, J.; Leathwick, J. R.; Hastie, T. A working guide to boosted regression trees. *J. Anim. Ecol.* **2008**, *77*, 802−813.
(38) Ridgeway, G. *Generalized boosted regression models*. Documentation on the R Package 'gbm', version 1·5−7. [Online], 2006, http://www.i-pensieri.com/gregr/gbm.shtml (accessed on April 1, 2008).
(39) Hijmans, R.; Phillips, S.; Leathwick J.; Elith, J. dismo: Species distribution modeling. R package version 0.8−11. [Online], 2012, http://CRAN.R-project.org/package=dismo (accessed on January 1, 2012).
(40) Swets, J. A. Measuring the accuracy of diagnostic systems. *Science.* **1998**, *240*, 1285−1293.
(41) Fawcett, T. An introduction to ROC analysis. *Pattern Recogn. Lett.* **2006**, *27*, 861−874.
(42) Robin, X.; Turck, N.; Hainard, A.; Tiberti, N.; Lisacek, F.; Sanchez, J.; Müller, M. pROC: An open-source package for R and S+ to analyze and compare ROC curves. *BMC Bioinform.* **2011**, *12*, 77.
(43) Mease, D.; Wyner, A.; Buja, A. Boosted classification trees and class probability/quantile estimation. *J. Mach. Learn. Res.* **2007**, *8*, 409−439.
(44) Flach, P.; Matsubara, E. On classification, ranking, and probability estimation. In *Probabilistic, Logical and Relational Learning—A Further Synthesis*; de Raedt, L., Dietterich, T., Getoor, L., Kersting, K., Muggleton, S., Eds.; Internationales Begegnungs- und Forschungszentrum fur Informatik (IBFI): Dagstuhl, Germany, 2008.
(45) Platt, J. Probabilistic outputs for support vector machines and comparison to regularized likelihood methods. In *Advances in Large Margin Classifiers*; Smola, A., Bartlett, P., Scholkopf, B., Schuurmans, D., Eds.; The MIT Press: Cambridge, MA, 2000.
(46) Niculescu-Mizil, A.; Caruana, R. Predicting good probabilities with supervised learning. I*n Proceedings of the 22nd International Conference on Machine Learning*, Bonn, Germany, 2005; de Raedt, L., Wrobel, S., Eds.; ACM: New York, NY, 2005; pp 625−632.
(47) Wallace, B.; Dahabreh, I. Improving class probability estimates for imbalanced data. *Knowl. Inf. Syst.* **2014**, *41* (1), 33−52.

DOI: 10.1021/es502579u
Environ. Sci. Technol. 2015, 49, 4354−4361